

Magnetic property measurements on single wall carbon nanotube polyimide composites

Keun J. Sun,¹ Russell A. Wincheski,^{2,a)} and Cheol Park¹

¹National Institute of Aerospace, 100 Exploration Way, Hampton, Virginia 23666, USA

²NASA-Langley Research Center, Hampton, Virginia 23681, USA

(Received 23 April 2007; accepted 18 November 2007; published online 22 January 2008)

Magnetization measurements as a function of temperature and magnetic field were performed on polyimide nanocomposite samples containing various weight percentages of single wall carbon nanotubes. It was found that the magnetization of the composite, normalized to the mass of nanotube material in the sample, decreased with increasing weight percentage of nanotubes. It is possible that the interfacial coupling between the carbon nanotube (CNT) fillers and the polyimide matrix promotes the diamagnetic response from CNTs and reduces the total magnetization of the composite. The coercivity of the samples, believed to originate from the residual magnetic catalyst particles, was enhanced and had stronger temperature dependence as a result of the composite synthesis. These changes in magnetic properties can form the basis of a new approach to investigate the interfacial properties in the CNT nanocomposites through magnetic property measurements.

© 2008 American Institute of Physics. [DOI: [10.1063/1.2832616](https://doi.org/10.1063/1.2832616)]

I. INTRODUCTION

Multifunctional nanocomposites prepared from single wall carbon nanotubes (SWCNTs) and polyimides are anticipated to have many aerospace applications. Nanocomposite films containing small amounts of well dispersed SWCNTs have been shown to possess enhanced electrical conductivity, mechanical strength, and thermal stability.¹ Theoretically, it has been derived that external magnetic fields have a strong effect on the electronic structure and bulk properties of carbon nanotubes (CNTs).^{2,3} A SWCNT can have either a paramagnetic or diamagnetic response to an applied magnetic field depending on the tube's diameter, chirality, Fermi energy level, and the direction of the magnetic field relative to tube axis. A SWCNT-polymer composite thus may have magnetic field sensing functions if a proper amount of SWCNTs are embedded in the polymer and the intrinsic properties of CNTs, which are sensitive to the applied magnetic field, can be measured. In addition to controllable dispersion, alignment of SWCNTs in a polymer matrix is a primary factor⁴ for maximizing the use of CNTs' exceptional mechanical properties in the reinforcement of a structure. Films of strong magnetic field aligned SWCNTs and SWCNT ropes have been produced^{5,6} and anisotropic behavior in some of their physical properties was characterized.⁷ Both in the magnetic alignment of SWCNTs for fabrication of a rope and in the magnetic alignment of SWCNTs and SWCNT ropes in polymers, the magnetic susceptibility of CNTs is one of the crucial parameters to determine the effectiveness of the applied magnetic field.

Raman spectroscopy has been used in the investigation of the elastic properties of SWCNTs in polymer composites^{4,8} and has been proposed as an approach to determine the residual strains and load transfer in the nanocomposites.⁴ A direct coupling of SWCNT to the poly-

mer matrix, instead of a van der Waals type mechanism, was suggested as the cause of the frequency shift of certain Raman modes. It is possible that the magnetic property of SWCNTs would also be affected by such a coupling and that measurement of the magnetic response could become another approach to nondestructively study the interfacial properties of a nanocomposite. Here we investigate the magnetic properties of the composites and changes in these properties with SWCNT concentration. It is hoped that the obtained results will be informative in the development of magnetic sensing capabilities within nanocomposites, for a feasibility study of *in situ* alignment of nanotubes while synthesizing composites, and in the refinement of SWCNT-polyimide nanocomposite fabrication techniques.

II. EXPERIMENTAL

Using a superconducting quantum interference device (Quantum Design, SQUID-MPMS system) magnetometer, magnetization measurements as a function of temperature at constant magnetic field and as a function of magnetic field at constant temperature were performed on single wall carbon nanotube polyimide composite films. Most of the measured samples differed in weight percentage of SWCNTs. Composites with 0.1%, 0.2%, 1%, 5%, 10%, and 20% SWCNTs were studied. The weights of the composite film samples were in the range of 3–50 mg, and thicknesses were between 23 and 81 μm . Magnetic properties of pure polyimide and pristine SWCNT samples were also measured to provide background information. Measurements were performed over temperatures in the range of 5–400 K and at magnetic fields up to 15 kOe. Data reproducibility was verified by either repeating the measurements on the same sample or conducting the same measurements on different samples made from the same batch of SWCNTs. Data consistency was also obtained by comparing the results of temperature dependence measurements with those of magnetic field de-

^{a)}Electronic mail: russell.a.wincheski@nasa.gov.

TABLE I. Weight percentage of SWCNTs in the measured polyimide composite samples.

Nanocomposite sample name	Weight percentage of SWCNTs (%)	Source of SWCNTs (HiPCO)	Sample thickness (μm)
A1	0.1	Batch A	58
B1	0.2	Batch B	44
B2	1	Batch B	69
B3	5	Batch B	81
B4	10	Batch B	23
C1	10	Batch C	46
D1	20	Batch D	38

pendence. There was very good agreement between the two sets of data in our measurements; experimental uncertainties were better than 1%. With exception of the 0.1% nanocomposite sample which had very small magnitude of magnetization (in the order of 10^{-5} emu), magnetization measurements of other samples had less than 0.5% experimental errors.

SWCNT-polyimide films were prepared starting with a dilute SWCNT (purified HiPCo, CNI) suspension, typically around 0.05 wt %, in *N,N*-dimethylacetamide (DMAc), which was sonicated overnight at 40 kHz. The sonicated SWCNT suspension was then used as a solvent for the poly(amic acid) synthesis with the diamine, 2,6-bis(3-aminophenoxy) benzonitrile [$(\beta\text{-CN})\text{APB}$], and the dianhydride, 4,4'-oxydiphthalic anhydride (ODPA). The entire reaction was carried out with stirring in a nitrogen purged flask immersed in a 40 kHz ultrasonic bath until the solution viscosity increased and stabilized. Sonication was stopped and stirring continued for several hours to form a SWCNT-poly(amic acid) solution. The solutions were cast on glass plates and cured to complete the imidization reaction to form thin SWCNT-polyimide (SWCNT/LaRC-EAP) films. Further details on the fabrication methodology are discussed in a previous report.¹

For this study, batches of SWCNTs from various sources were used for fabricating the nanocomposites. The 0.1% nanocomposites employed batch A SWCNTs, the 0.2%, 1%, 5%, and 10% composites used batch B SWCNTs, another 10% sample was fabricated with batch C, and the 20% composite used batch D SWCNTs. Different batches were either obtained from different sources or prepared with a slightly different process than other batches from a single source. The names and characteristics of the samples are summarized in Table I. Two additional nanotube sources, batches E and F, were also examined, although limited quantities of these sources precluded composite material fabrication. It should be noted that batches A–E are HiPCO carbon nanotubes. Iron particles were employed as the catalyst in the process for the growth of these carbon tubes.^{9–11} Batch F carbon nanotubes were made by a laser ablation method with cobalt and nickel as catalysts. Although all samples were subjected to a purification process, low weight percentages of magnetic particles still remained in the samples. Variations in size and concentration of the remaining iron particles were found to result in a large batch to batch variation in the measured magnetic properties of the composite samples.

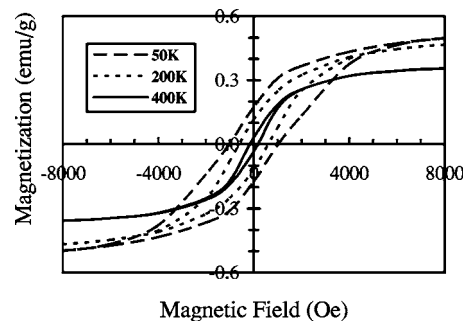


FIG. 1. Magnetic field dependent magnetization curves of sample C1 at temperatures of 50, 200, and 400 K. The curves exhibit the typical hysteresis behavior of a ferromagnet. The coercivity is still significant up to 400 K.

However, for the composites synthesized with various percentages of SWCNTs from a single nanotube batch, changes in the magnetic properties as a function of doping concentration were also observed and may yield important information on the coupling of the tube to the matrix.

III. RESULTS AND DISCUSSION

Nanocomposites had shown significant changes in some magnetic properties from their constituent SWCNTs. Results of the coercivity and the magnetization of batches A–D composite samples will be presented and discussed. Magnetic susceptibility of batches E and F SWCNTs, which had a much lower percentage of magnetic residues than batches A–D, will be analyzed in the latter section. In the following figures and discussions, unless it is indicated otherwise, emu/g is the unit that represents the magnetization per gram of the SWCNT batch, which includes the mass of SWCNTs and magnetic residues.

A. Nanocomposites

The magnetization of batches C and D nanocomposite films was measured at temperatures in the range of 10–400 K. Variation in coercivity with temperature was quite substantial. Figure 1 shows the magnetization curves of the 10% batch C nanocomposite film sample (C1) at temperatures of 50, 200, and 400 K. The curves show the typical hysteresis loop of a ferromagnetic material. Both the saturation magnetization and the coercivity increased as temperature decreased. At a magnetic field of 8 kOe, the composite had a magnetization of 0.356 emu/g of the composite at 400 K, increasing to 0.513 emu/g at 50 K. Coercivity of the sample was quite significant up to 400 K, measured as 95 and 1055 Oe at temperatures of 400 and 50 K, respectively. The coercivity of batch C bare nanotubes was slightly over a hundred oersteds at 100 K and had a much smaller temperature dependence than that found for the composite sample C1 (912 Oe at 100 K). This increase in coercivity of the SWCNTs upon incorporation into the composite may well be the result of interfacial couplings between the SWCNTs and polymers. The 20% batch D composite sample D1 had similar characteristics to sample C1. Magnetization data of this

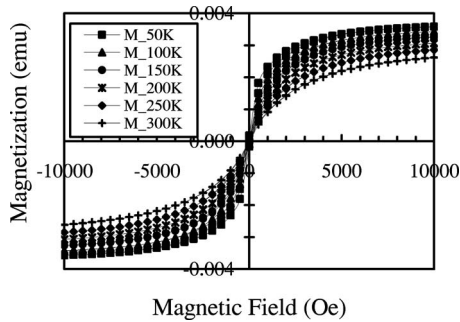


FIG. 2. Magnetization as a function of magnetic field of sample B3 measured at constant temperatures. Saturation magnetization increases with the decrease of sample temperature. No coercivity is observed at temperatures above 100 K.

sample showed an increase in coercivity from approximately 137 Oe at 400 K up to 1001 Oe at 50 K and 1290 Oe at 10 K.

Figure 2 shows the magnetization curves of the B3 (5% SWCNT) composite sample at different temperatures. Contrary to samples C1 and D1, sample B3 displayed negligible hysteresis for sample temperature at or above 100 K. Taking the measurement uncertainty into account, the coercivity was essentially zero at these temperatures. While the saturation magnetization increased with decreasing temperatures from 400 to 10 K, measurable coercivity was not present until the sample temperature was lowered below 100 K. Furthermore, the magnetization curves of sample B3 measured at different temperatures superimposed when plotted as a function of H/T (Fig. 3). These data suggest that the size of residual catalyst particles in batch B nanotubes is less than the critical diameter for superparamagnetism to occur.¹² Measurements of pristine batch B nanotubes and composite samples of other weight percentage of batch B nanotubes showed similar magnetic field dependence.

Figure 4 illustrates the magnetization as a function of temperature at a magnetic field of 10 kOe for sample B2 (1%). The magnetization is seen to increase nearly linearly with decreasing temperature across the measurement range. This behavior is in contrast to the molecular field theory of a ferromagnet that predicts a constant magnetization as the temperature approaches 0 K.¹³ This unusual behavior was observed for all the other nanocomposite samples. Although

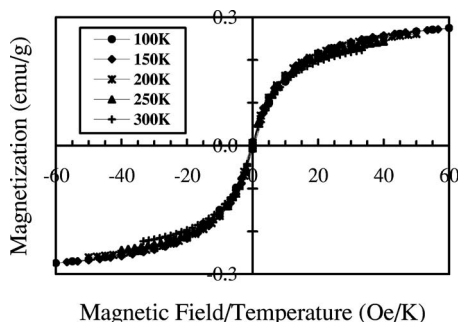


FIG. 3. Magnetization as a function of magnetic field/temperature (H/T) for sample B3 at constant temperatures. Overlapping of curves could imply that magnetic particles, which are responsible for the magnetization, are of very fine size and have single magnetic domain.

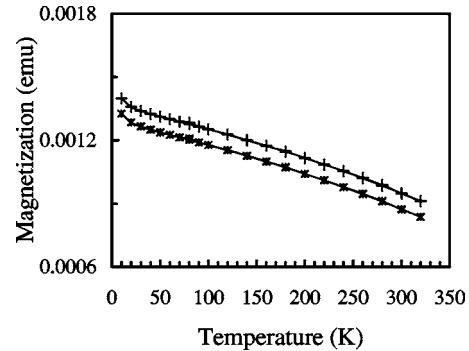


FIG. 4. Temperature dependent magnetization of 1% batch B composite sample (sample B2) at magnetic field of 10 kOe. Curve on the top is the magnetization response of batch B SWCNTs in the composite after magnetization contributed by the polyimide was subtracted from the raw data (bottom curve).

oxygen gas undergoes a magnetic phase transition¹⁴ from diamagnetic to paramagnetic at 57 K, the transition alone does not account for the increasing magnetization with decreasing temperature shown in Fig. 4. Correcting for the magnetization of the polyimide in the composite also did not explain the magnetization behavior of the SWCNTs in the composite. As the pure polyimide displayed a small diamagnetic response at all temperatures, this correction merely resulted in a slight increase in the magnetization attributed to batch B SWCNTs.

In performing data analysis, the properties of the initial nanotube batch must be taken into account. Figure 5 shows the measured magnetization as a function of magnetic field at 100 K for four bare SWCNT samples from four different batches. Both the saturation magnetization and coercivity of the CNTs are heavily batch dependent. A CNT nanocomposite synthesized with SWCNTs with large coercivity would be expected to have greater coercivity than a nanocomposite synthesized from a lower coercivity SWCNT batch. For composites made with SWCNTs from the same batch, however, changes in coercivity with nanotube weight percentage can be measured. Figure 6 displays the temperature dependent coercivity of samples B1, B2, B3, B4, and C1. The coercivity of sample C1 is at least an order of magnitude higher than batch B samples for the temperatures above 20 K. This increased coercivity of sample C1 over batch B samples is directly related to the coercivity of the bare nano-

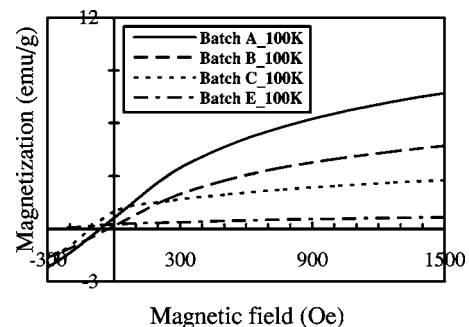


FIG. 5. Magnetization of different batches of SWCNTs at 100 K. Not only the saturation magnetization but also the coercivity varies from batch to batch.

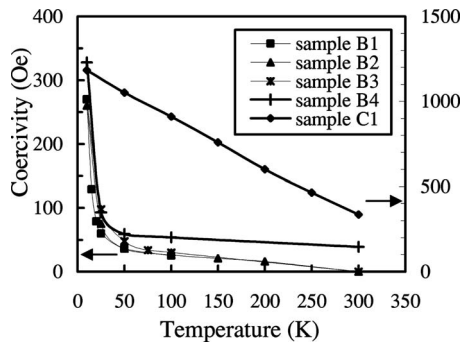


FIG. 6. Temperature dependence of coercivity of samples B1, B2, B3, B4, and C1 (from bottom to top). Magnetic properties of the nanocomposites are mostly determined by their component SWCNTs/iron particles.

tubes shown in Fig. 5. Batch B nanotubes and their nanocomposites show zero or close to zero coercivity at high temperatures, turning sharply to higher values for $T < 20$ K. At these low temperatures, the coercivity increases with SWCNT weight percentage. This increase in coercivity with SWCNT weight percentage is likely caused by the occurrence of an aggregation of nanotubes. Uniform dispersion of carbon nanotubes in polymers becomes more difficult as the SWCNT weight percentage increases, increasing the potential for aggregate formation. Long-range interactions among magnetic particles within an aggregation of SWCNTs can then be developed and become effective at restraining the motions of the magnetic moments of the particles.

Electron spin resonance¹⁵ and thermogravimetric analysis (TGA) analysis of the SWCNTs used in this study confirmed the presence of iron residue in the SWCNT batches. Magnetic saturation measurements can be used to estimate the wt % of iron in the nanocomposites by assuming that the saturation magnetization is dominated by the residual magnetic particles in the samples. Such measurements have been performed using a SQUID magnetometer with the results showing a residual iron content of 1.5%–4.1% in the batches A–D of SWCNTs. Since there is no expectation that carbon nanotubes would have a magnetic domain structure, it is plausible to assume that the iron particles are responsible for the magnetic hysteresis and, thus, the coercivity in the composites. Experimental data reveal that the coercivity of the SWCNT material is altered upon fabrication into the nanocomposite. A higher coercivity and a much stronger temperature dependence are seen in the nanocomposites as compared to the bare SWCNTs. Changes in stress on the surface of the iron particles, due to the synthesis with the polyimide, may result in the increased coercivity and the stronger temperature dependence. Stress induced changes of SWCNTs upon fabrication into nanocomposites have been reported in the past^{4,8} and help to substantiate this theory.

Fine and single-domain magnetic particles are known to possess superparamagnetic behavior above certain temperatures.¹² When the magnetization and/or anisotropic energy of these particles are of the same order of magnitude as the thermal fluctuation energy, magnetic moments become randomly oriented in the absence of an external magnetic field. The magnetic remanence is insignificant and no coercivity is observed. When the temperature is lowered, thermal

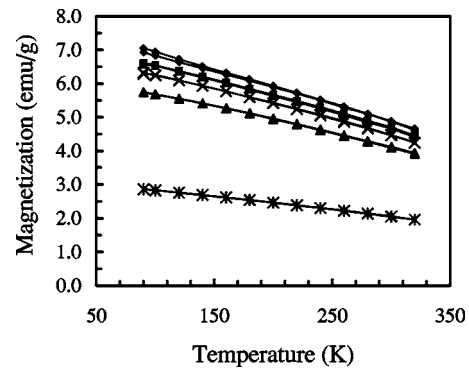


FIG. 7. Temperature dependent magnetization of batch B SWCNTs and batch B nanocomposites. Curves from top to the bottom are the magnetization at 6 kOe for batch B nanotubes (curve with \blacklozenge), and composite samples B1 (0.2%, \blacksquare), B2 (1%, \times), B3 (5%, \blacktriangle), and B4 (10%, $*$), respectively. Magnetization (normalized by per gram of SWCNT batch) decreases with increasing weight percentage.

energies are reduced and internal magnetic interactions, such as magnetocrystalline interactions, become predominant. As a result, magnetic order will be retained in the sample as the external magnetic field is removed. This effect was observed for batch B SWCNT composites in this study, with a superparamagnetic critical temperature of 100 K. Although it was difficult to accurately measure the size of the iron particles embedded in the composite, high resolution scanning electron microscopy of batch B bare SWCNTs did reveal that the iron residues were less than 5 nm in diameter.

Given the particle size, a measurement of the superparamagnetic critical temperature provides a method for determining the magnetic anisotropic energy of the particle. The magnetic anisotropy energy E_a of the iron particles can then be estimated from equation¹²

$$E_a = 25K_B T_B \langle V \rangle,$$

where K_B is Boltzmann's constant, T_B is the blocking temperature of the superparamagnetism (assumed to be 100 K for batch B composite samples), and $\langle V \rangle$ is the volume of the particle. Using 5 nm as the maximum diameter of the iron particles in the polyimides results in an estimate of $E_a \geq 5.27 \times 10^6$ ergs/cm³, an order of magnitude larger than that of an isolated iron particle.¹³ Several factors including magnetocrystalline interactions, surface stress of the particle, shape of the particle, and dipole-dipole magnetic interactions between the particles can contribute to the anisotropy energy of a nanosize magnetic particle. In the present study with the low weight percentage SWCNT-polyimide samples and spherical magnetic particles, it is believed that the anisotropy energy arises mainly from the magnetocrystalline interactions and is enhanced by the polymer induced surface stresses on the particles. There have been discussions on the changes in size and in magnetic properties of iron particles before and after the SWCNT growth¹⁶ and of iron oxide nanocrystals synthesized in a polymer matrix.¹⁷ The increase in anisotropy energy estimated here for batch B samples is consistent with the findings of the previous works.

The saturation magnetization of batch B SWCNTs and nanocomposites as a function of temperature is displayed in Fig. 7. In this plot, the effect of the pure polyimide has been

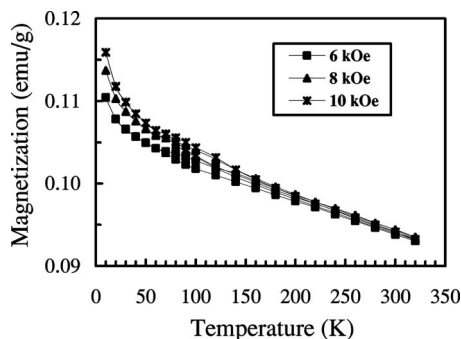


FIG. 8. Temperature dependent magnetization of batch F SWCNTs at fields of 6, 8, and 10 kOe. The increase of magnetization at low temperatures could be attributed to the paramagnetism of the SWCNTs.

subtracted to obtain the response due solely to the nanotubes/iron particles in the sample. For each sample, the magnetization increased with decreasing temperature. The rate of increase was smaller for the samples with higher loading of SWCNTs. In addition, at each temperature, the magnetization decreased as the weight percentage of SWCNTs increased. A decrease in magnetization of the SWCNTs after synthesis with polyimides was also observed for samples of A1, C1, and D1. A coupling between the nanotubes and polymer was expected¹⁸ and appears to not only increase the surface stress on the iron particles (resulting in increased sample coercivity) but also to influence the magnetic properties of the CNTs. The interfacial coupling between the carbon nanotubes and the polyimides appears to promote the diamagnetic response from the CNTs and thus reduce the total magnetization of the composite. The reason for the systematic decrease of magnetization with increasing weight percentage, however, is not yet completely clear.

B. Magnetic responses of low magnetic particle concentration SWCNTs

SWCNTs can have large paramagnetic or diamagnetic responses to an applied magnetic field.^{2,3} The predominant role of the residual iron particles made it difficult to directly measure the magnetic response from the nanotubes in batches A–D of SWCNTs and their composite film samples. For the SWCNT samples with very low percentages of magnetic particles, however, the magnetic properties of the SWCNTs could be inferred from temperature dependent magnetization measurements with some intriguing results.

The weight percentage of magnetic residues calculated from magnetic saturation measurement for batch E and batch F SWCNTs was estimated to be 0.3% and less than 0.1%, respectively. Figure 8 displays the temperature dependent magnetization of batch F SWCNTs at 6, 8, and 10 kOe. For each field, magnetization data were collected in a thermal cycle from 320 to 10 K and back to 320 K. There was thermal hysteresis for the magnetization at temperatures between 200 and 70 K with a smaller magnetization during the cooling cycle. At room temperatures, the magnetization of the sample is saturated at 6 kOe. The magnetization is believed to be contributed predominantly by the saturated magnetic moments of residual catalyst particles. As the sample temperature was lowered, magnetization is seen to continue to

increase. Below 200 K, the three sets of curves started to diverge. Similar results were obtained for batch E SWCNTs. Along with a larger residual catalyst content, batch E showed a much larger coercivity (300 Oe at room temperature). The two batches were in powder form and each had a mass of less than 10 mg. As calculated from the data, the paramagnetic susceptibility increased with decreasing temperatures. For the samples from batch F, the averaged susceptibilities were 3×10^{-7} , 1.37×10^{-5} , and 5.24×10^{-5} emu/g at 300, 100, and 10 K, respectively. For batch E, a much larger susceptibility (1.3×10^{-5} emu/g) was obtained at 300 K, probably due to a larger size of the ferromagnetic particles in this batch. Susceptibilities at low temperatures are close to the values of batch F SWCNT samples.

It is difficult to account for the observed magnetic properties of batches E and F SWCNTs based solely upon residual magnetic particles in the samples. Fine ferromagnetic particles alone would not be expected to show a continuous increase in magnetization at high magnetic field and in magnetic susceptibility as sample temperature is decreased. It is proposed here that an induced magnetization of the metallic carbon nanotubes contributes substantially to that of the ferromagnetic catalyst particles in these samples. Evidence of such a magnetic response of carbon nanotubes to an applied field has been documented in the literature. Recently, there was a report¹⁹ on the induced magnetism in carbon nanotubes by contacting the nanotubes with magnetic materials. A visualization of dispersed SWCNTs in a polymer matrix via magnetic force microscopy (MFM) has also been reported.²⁰ Finally, it has been found in the fabrication of CNT electronic devices that the magnetic susceptibility of CNTs can be increased through the use of adhered ferromagnetic nanoparticles.²¹

IV. SUMMARY

Magnetization measurements were performed on composite films of various weight percentages of SWCNTs in polyimides. The composites, except those showing superparamagnetic behavior, had enhanced coercivity and stronger temperature dependence of coercivity than the constituent SWCNTs. It was also observed that the saturation magnetization of the composites decreased with increasing weight percentage of SWCNTs. Magnetic properties of the composites were largely affected by magnetic particles which were used as catalysts for the growth of CNTs and remained with the CNTs during processing and synthesis of the nanocomposites. An increase in coercivity of the composites over constituent SWCNTs was measured and is believed to be induced by the surface stress on the iron particles due to synthesis within the polymer.^{4,17} The same type of coupling between the carbon nanotubes and polymer is believed to be responsible for the increased diamagnetic effects from SWCNTs and resulted in a decrease of magnetization per gram of the SWCNTs with increasing SWCNT weight percentage. Coupling between the carbon nanotubes and the polyimides play an important role in determining the mechanical strength of a nanocomposite. Investigating changes in the magnetic properties of SWCNTs in the polymer matrix

may provide a unique tool for the study and characterization of interfacial interactions between the component materials in a nanocomposite.

SWCNT batches with low percentage of iron residues showed increasing magnetic susceptibility with decreasing temperature, which may be caused by the contribution from magnetized iron residues coupling with paramagnetic SWCNTs. Optimization of such an interaction would be beneficial to the development of nanotube based magnetic field sensors and in the magnetic alignment of nanotube based materials.

ACKNOWLEDGMENTS

The authors would like to thank Dr. P. Lillehei for providing the SEM particle size analysis, and Dr. P. Williams, D. Perey, and Dr. E. J. Siochi for their review and comments on this article. They also would like to thank Dr. Sivaram Arepalli and Dr. Len Yowell at NASA Johnson Space Center and Dr. David Geohegan at Oak Ridge National Laboratory for providing purified batch E and F SWCNTs, respectively. C. P. appreciates NASA University Research, Engineering and Technology Institute on Bio Inspired Materials (BIMat) under Award No. NCC-1-02037 for support in part.

¹C. Park, Z. Ounaies, K. A. Watson, R. E. Crooks, J. Smith, Jr., S. E. Lowther, J. W. Connell, E. J. Siochi, J. S. Harrison, and T. L. St. Clair, *Chem. Phys. Lett.* **364**, 303 (2002).

²J. P. Lu, *Phys. Rev. Lett.* **74**, 1123 (1995).

³H. Ajiki and T. Ando, *J. Phys. Soc. Jpn.* **62**, 2470 (1993).

⁴V. G. Hadjev, M. N. Iliev, S. Arepalli, P. Nikolaev, and B. S. Files, *Appl. Phys. Lett.* **78**, 3193 (2001).

⁵D. A. Walter, M. J. Casavant, X. C. Quin, C. B. Huffman, P. J. Boul, L. M. Ericson, E. H. Haroz, M. J. O'Connell, K. Smith, D. T. Colbert, and R. E. Smalley, *Chem. Phys. Lett.* **338**, 14 (2001).

⁶B. W. Smith, Z. Benes, D. E. Luzzi, J. E. Fischer, D. A. Walter, M. J. Casavant, J. Schmidt, and R. E. Smalley, *Appl. Phys. Lett.* **77**, 663 (2000).

⁷J. Hone, M. C. Liaguno, N. M. Nemes, A. T. Johnson, J. E. Fischer, D. A. Walter, M. J. Casavant, J. Schmidt, and R. E. Smalley, *Appl. Phys. Lett.* **77**, 666 (2000).

⁸M. D. Frogley, Q. Zhao, and H. D. Wagner, *Phys. Rev. B* **65**, 113413 (2002).

⁹P. Nikolaev, M. J. Bronikowski, R. K. Bradley, F. Rohmund, D. T. Colbert, K. A. Smith, and R. E. Smalley, *Chem. Phys. Lett.* **313**, 91 (1999).

¹⁰M. J. Bronikowski, P. A. Willis, D. T. Colbert, K. A. Smith, and R. E. Smalley, *J. Vac. Sci. Technol. A* **19**, 1800 (2001).

¹¹I. W. Chiang, B. E. Brinson, A. Y. Huang, P. A. Willis, M. J. Bronikowski, J. L. Margrave, R. E. Smalley, and R. H. Huang, *J. Phys. Chem. B* **105**, 8297 (2001).

¹²B. D. Cullity, *Introduction to Magnetic Materials* (Addison-Wesley, Reading, MA, 1972), p. 410.

¹³C. Kittel, *Introduction to Solid State Physics*, 3rd ed. (Wiley, New York, 1966).

¹⁴S. Gregory, *Phys. Rev. Lett.* **40**, 723 (1978).

¹⁵(Private Communication).

¹⁶R. A. Harutyunyan, T. Tokune, E. Mora, J.-W. Yoo, and A. J. Epstein, *J. Appl. Phys.* **100**, 044321 (2006).

¹⁷J. K. Vassiliou, V. Mehrotra, M. W. Russell, R. D. McMichael, R. D. Shull, and R. F. Ziolo, *J. Appl. Phys.* **73**, 5109 (1993).

¹⁸S. A. Curran, P. M. Ajayan, W. J. Blau, D. L. Carroll, J. A. Coleman, A. B. Dalton, A. P. Davey, A. Drury, B. McCarthy, S. Maier, and A. Strevens, *Adv. Mater.* **10**, 1091 (1998).

¹⁹O. C'espedes, M. S. Ferreira, S. Sanvito, M. Kociak, and J. M. D. Coey, *J. Phys.: Condens. Matter* **16**, L155 (2004).

²⁰P. Lillehei, J. Rouse, C. Park, and E. J. Siochi, *Nano Lett.* **2**, 827 (2002).

²¹D. P. Long, J. L. Lazorcik, and R. Shashidhar, *Adv. Mater.* **16**, 814 (2004).